

Evolution and Energization of Energetic Electrons in the Inner Magnetosphere

15 January 2009

Joseph F. Fennell and James L. Roeder
Space Science Applications Laboratory
Physical Sciences Laboratories

Prepared for

Space and Missile Systems Center
Air Force Space Command
483 N. Aviation Blvd.
El Segundo, CA 90245-2808

Authorized by: Engineering and Technology Group

20090227366

APPROVED FOR PUBLIC RELEASE;
DISTRIBUTION UNLIMITED

This report was submitted by The Aerospace Corporation, El Segundo, CA 90245-4691, under Contract No. FA8802-09-C-0001 with the Space and Missile Systems Center, 483 N. Aviation Blvd., El Segundo, CA 90245. It was reviewed and approved for The Aerospace Corporation by J. H. Clemmons, Principal Director, Space Science Applications Laboratory; and D. C. Marvin, Principal Director, Research and Program Development Office. Col. David E. Swanson was the project officer for the Mission-Oriented Investigation and Experimentation (MOIE) program.

This report has been reviewed by the Public Affairs Office (PAS) and is releasable to the National Technical Information Service (NTIS). At NTIS, it will be available to the general public, including foreign nationals.

This technical report has been reviewed and is approved for publication. Publication of this report does not constitute Air Force approval of the report's findings or conclusions. It is published only for the exchange and stimulation of ideas.

Approved for public release
per SMC/PA file #08-557

Col. David E. Swanson
SMC/EA

REPORT DOCUMENTATION PAGE			<i>Form Approved</i> <i>OMB No. 0704-0188</i>		
<small>Public reporting burden for this collection of information is estimated to average 1 hour per response, including the time for reviewing instructions, searching existing data sources, gathering and maintaining the data needed, and completing and reviewing this collection of information. Send comments regarding this burden estimate or any other aspect of this collection of information, including suggestions for reducing this burden to Department of Defense, Washington Headquarters Services, Directorate for Information Operations and Reports (0704-0188), 1215 Jefferson Davis Highway, Suite 1204, Arlington, VA 22202-4302. Respondents should be aware that notwithstanding any other provision of law, no person shall be subject to any penalty for failing to comply with a collection of information if it does not display a currently valid OMB control number. PLEASE DO NOT RETURN YOUR FORM TO THE ABOVE ADDRESS.</small>					
1. REPORT DATE (DD-MM-YYYY) 15-01-2009		2. REPORT TYPE		3. DATES COVERED (From - To)	
4. TITLE AND SUBTITLE Evolution and Energization of Energetic Electrons in the Inner Magnetosphere			5a. CONTRACT NUMBER FA8802-09-C-0001		
			5b. GRANT NUMBER		
			5c. PROGRAM ELEMENT NUMBER		
6. AUTHOR(S) Joseph F. Fennell and James L. Roeder			5d. PROJECT NUMBER		
			5e. TASK NUMBER		
			5f. WORK UNIT NUMBER		
7. PERFORMING ORGANIZATION NAME(S) AND ADDRESS(ES) The Aerospace Corporation Physical Sciences Laboratories El Segundo, CA 90245-4691			8. PERFORMING ORGANIZATION REPORT NUMBER TR-2009(8550)-4		
9. SPONSORING / MONITORING AGENCY NAME(S) AND ADDRESS(ES) Space and Missile Systems Center Air Force Space Command 483 N. Aviation Blvd. El Segundo, CA 90245			10. SPONSOR/MONITOR'S ACRONYM(S) SMC		
			11. SPONSOR/MONITOR'S REPORT NUMBER(S)		
12. DISTRIBUTION/AVAILABILITY STATEMENT Approved for public release; distribution unlimited.					
13. SUPPLEMENTARY NOTES					
14. ABSTRACT A review is presented of what we know about the evolution and energization of energetic electrons in the inner magnetosphere. We emphasize what we have learned since the review by Friedel et al. (2002) with the primary result being a greater focus on local acceleration processes and significant new evidence that points to processes that are acting in the region between GPS and geosynchronous altitudes. We use as an example the magnetosphere's energetic electron responses to storms that occurred in the 16–25 July 2004 period. They had increasing magnitude in terms of minimum D_{ST} of –80, –101, –148, and –197 nT. We examined the penetration and enhancements of the electrons as a function of L . We found that the smallest storms did not cause relativistic electron enhancements for $L < 6.5$, but did cause enhancements in the “source” populations at >130 and >230 keV down to $L \sim 3.0$. The results indicate that the electron fluxes observed at Cluster may be directly linked to the rapid response of electrons at low L observed by HEO3, and could have been the source for the <1 MeV fluxes.					
15. SUBJECT TERMS Space radiation, Radiation belts, Electron energization, Inner magnetosphere					
16. SECURITY CLASSIFICATION OF:			17. LIMITATION OF ABSTRACT	18. NUMBER OF PAGES 26	19a. NAME OF RESPONSIBLE PERSON Joe Fennell
a. REPORT UNCLASSIFIED	b. ABSTRACT UNCLASSIFIED	c. THIS PAGE UNCLASSIFIED			19b. TELEPHONE NUMBER (Include area code) (310)336-7075

Acknowledgments

The authors would like to acknowledge their many colleagues at The Aerospace Corporation that have supported their efforts, provided references, and participated in discussions on the topic of energetic electron sources and process in the magnetosphere. This work was supported by grant GC189637NGA from Boston University and by The Aerospace Corporation's Mission-Oriented Investigation and Experimentation program.

Contents

1.	Introduction	1
2.	What Has Been Learned?	3
	2.1 Parameters Used in This Report	3
	2.2 Summary of Current Knowledge	3
	2.3 Radial Transport and M Violation Processes	5
	2.4 Peak Electron Enhancements and Phase Space Density Dependences With L	5
	2.5 Source Populations	8
3.	Energetic Electron Responses During July 2004 Storms	11
	3.1 Data Sources for Example Storms	11
	3.3 Cluster Observations of July 24, 2004 Storm	15
4.	Summary	19
	References	21

Figures

1.	Example of the MeV electron flux dependence on solar wind velocity	1
2.	Examples of MeV electron flux dropouts and post-storm gains over a range of L values (panel a) and the evolution of the pitch angle distributions during the flux rise for three electron energies (panel b)	4
3.	Cartoon showing examples of relativistic electron PSD radial profiles for different transport and acceleration assumptions	6
5.	Location of the peak MeV electron fluxes as a function of storm minimum D_{ST}	7
6.	PSD radial profiles from Multisatellite observations during storm main and recovery phases plus comparisons to average PSD profiles	9
7.	PSD radial profiles for small (panel [a]) and moderate K values (panel [b])	10

8. D_{ST} , L_{pp} , and K_p for the period 14 July to 8 August in 2004	12
9. Coded electron intensity plots	13
10. Interplanetary magnetic field (top four panels).....	14
11. Spectrograms of spin-averaged electron fluxes measured by RAPID IES on all four Cluster spacecraft for 24 July 2004.....	16
12. Cluster 3 magnetic field measurements (top panel), energy-time spectrogram of RAPID IES spin averaged fluxes on C3 (second panel), and RAPID IES angular distributions from all four Cluster spacecraft (bottom four panels) for the interval 1530-2400 UT on 24 July 2004.....	17

1. Introduction

We have known for some time now that the outer zone electron fluxes respond to changes in solar wind conditions (Williams, 1966, Paulikas and Blake, 1976, 1979; Baker et al. 1978, 1986, 1994; Blake et al. 1997). In particular, high-speed solar wind streams correlate with electron fluxes increases, as do magnetic storm occurrences. Figure 1 shows an example of the relationship between solar wind velocity and >1.55 MeV electron fluxes taken at geosynchronous orbit (Paulikas and Blake, 1979). However, we also know that electron flux enhancements do not occur with all solar wind speed increases nor with all magnetic storms. Generating energetic electron flux increases may require a substantial solar wind speed increase associated with a precursor solar wind density enhancement combined with a southward turning of the IMF as was shown in Blake et al. (1997). Reeves et al. (2003) showed that magnetic storms could produce cases of energetic electron flux increases, decreases, or no change in flux. They also showed that, during an 11-year period in which they examined 226 storms, $\sim 53\%$ were followed by flux enhancements, $\sim 28\%$ were associated with flux decreases, and $\sim 19\%$ showed no change in the electron fluxes or an adiabatic response. They indicated that the magnitude of the storms, as measured by the minimum D_{ST} , did not matter, nor did the L value of the observations for $L < 7$; however, other evidence may be in disagreement with that

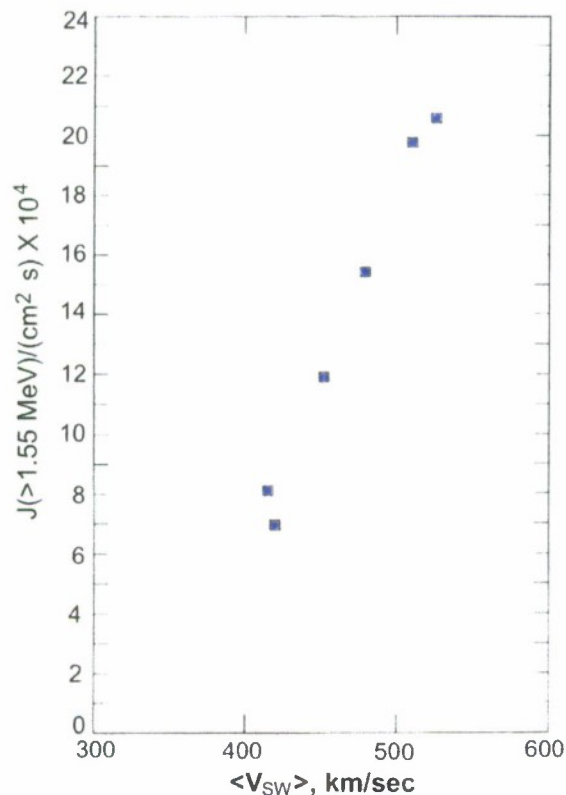


Figure 1. Example of the MeV electron flux dependence on solar wind velocity.

conclusion (see Tverskaya, et al., 2002; O'Brien et al., 2003). Like Paulikas and Blake (1979), Reeves et al. (2003) did note that the solar wind speed mattered and the flux increases were greater for larger speeds. Studies have also been made examining the source location of relativistic electrons (Selesnick and Blake, 2000), evolution of the energetic electron pitch angle distributions during post-storm flux enhancements (Blake et al., 2001; Horne et al., 2003), the relationship between the L value of the peak electron flux with storm magnitude (Tverskaya, et al. 2003) and plasma pause position (O'Brien and Moldwin, 2003), and the main phase and post-storm acceleration and losses of electrons (e.g. Horne et al., 2005; Meredith et al., 2002, 2003, 2006; O'Brien, et al., 2003; Shprits and Thorne, 2004; Shprits, et al., 2006; Thorne et al., 2005, etc.)

2. What Has Been Learned?

2.1 Parameters Used in This Report

Throughout this report, we will use L to identify the McIlwain (1961) L parameter that is computed by tracing a particle's trajectory between mirror points at the observation magnetic longitude in a model field. We will use L^* to indicate the Roederer (1970) L value that is computed by tracing the closed drift trajectory for an electron in a model field and is related to the magnetic flux enclosed by the particle's drift path. The reason for using both L and L^* is that not all storm-time studies used L^* , and the two parameters are not equivalent. We use K to represent the Kaufman (1965) K parameter, which is a representation of the second adiabatic invariant. Finally, we use M to indicate a particle's magnetic moment, the first adiabatic invariant. For more details on these parameters, see the references noted, or refer to Schulz and Lanzerotti (1974).

2.2 Summary of Current Knowledge

We have learned much from the observations quickly summarized in the introduction above. In particular, we have learned that the storm-time electron flux characteristics can be summarized as follows:

- (1) During the main phase of magnetic storms, there is a dropout of the relativistic electron fluxes as shown in Figure 2a, which is also often energy dependent (McAdams and Reeves, 2000; Meredith et al., 2002; Onsager et al., 2002) while at lower energies, the fluxes may actually increase. The loss was not an adiabatic response (McAdams and Reeves, 2000). Such losses are possibly due to microbursts, EMIC waves, strong chorus and hiss waves, and outward diffusion to the magnetopause or a combination thereof (Horne et al., 2003, 2005; Lorentzen et al., 2001; Shprits, et al., 2006; Thorne et al., 2005) while the increases at lower energies may result from convection or substorm injections.
- (2) The relativistic electrons start to increase at the beginning of the storm recovery phase, with increases at all pitch angles, but beginning earlier at the near-90° pitch angles, as shown in Figure 2b (Blake et al., 2001). The pitch angle distributions are more peaked during the acceleration phase than at other times, with the steepest distributions at injection/acceleration onset during the flux rise.
- (3) The increase in electron intensity and the flattening of the pitch angle distributions are relatively rapid at 1 MeV, with both features changing more slowly with increasing energy (see Figure 2b).
- (4) The steepness of the pitch angle distributions remains energy-dependent even after the intensity of the relativistic electrons ceases to increase (again Figure 2b).

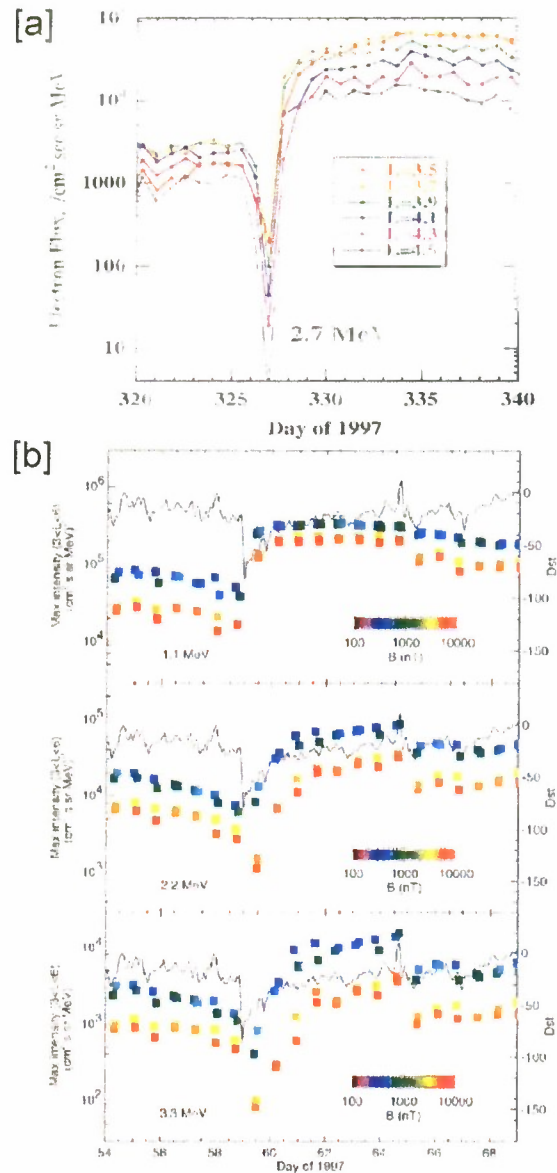


Figure 2. Examples of MeV electron flux dropouts and post-storm gains over a range of L values (panel a) and the evolution of the pitch angle distributions during the flux rise for three electron energies (panel b). The D_{ST} history is over-plotted on the pitch angle plots for reference. The pitch angle dependence of the fluxes is color coded to represent the field intensity at the particle mirror points. The pitch angle distribution is relatively flat when the red and blue points are close together (i.e., have nearly the same flux), and the distributions are peaked at 90° when the red and blue points are widely separated (after Blake et al., 2001).

- (5) The electron fluxes increase most rapidly in the vicinity of the L value, where the peak flux is finally established (Tverskaya et al., 2003; Blake et al., 2001).

- (6) Bursty, strong precipitation is intimately associated with the injection and acceleration of relativistic electrons (O'Brien et al., 2003).

2.3 Radial Transport and M Violation Processes

Friedel et al. (2002), in their review of electron dynamics in the inner magnetosphere, cited at least nine different mechanisms for generating relativistic electrons in the outer radiation belts. In all cases, the models generally assume a seed population of 100-keV electrons provided by substorms and convection. A coarse summary of the processes is that they either conserve or violate magnetic moment (M) conservation, the first adiabatic invariant.

Simple radial diffusion by ULF waves from high phase space density (PSD) regions into low PSD regions conserves M (Falthammer, 1968; Summers and Ma, 2000). Similarly, the enhanced radial diffusion discussed by Elkington et al. (1999, 2003) and Hudson et al. (1997, 2001) conserves M ; however, they used the known day-night asymmetry of the geomagnetic field to obtain faster transport rates than predicted for azimuthally symmetric field models. The main issue is whether radial transport alone is sufficient to account for the population and maintenance of the electron radiation belts. Fujimoto and Nishida (1990) tried to address this issue with a variation on radial diffusion that allowed pitch angle transport and recirculation of electrons to enhance the energy gained. That processes essentially required multiple cycles of radial transport inward near the equator to gain energy and outward well off the equator while conserving energy in the pitch angle transport process.

In the trapping region, violation of M can occur by electron cyclotron resonance with different plasma waves or by field-aligned curvature scattering. Doppler-shifted cyclotron resonance of electrons with ULF waves can occur during their bounce motion, as discussed by Summers and Ma (2000). Doppler-shifted cyclotron resonance with ELF/VLF waves from chorus, EMIC, and AKR, plus Landau resonance with magnetosonic waves, can violate M (Horne et al., 2003, 2005, 2007; Thorne et al., 2007; Meredith et al., 2002a,b; and others). Young et al., (2002; 2008) discussed and modeled the violation of M by changes in-field line curvature during storm times. In general, violation of M can lead to either acceleration or loss of electrons, but the field line curvature violation is only a loss process.

2.4 Peak Electron Enhancements and Phase Space Density Dependences With L

It has not been demonstrated, at this point, whether the M conserving and violating processes act alone or in concert to generate the resulting electron flux enhancements and the post-storm PSD profiles that are observed. However, radial transport and diffusion provides a good starting place from an observational perspective. It predicts a form for the electron PSD radial profiles that is easily observed by spacecraft that cover a significant range of L and L^* values. This classic PSD versus L^* form is shown schematically in Figure 3a. There is some long-standing evidence that diffusive and convective radial transport does occur, as evidenced by the many observations of a positive PSD gradient from small to large L^* (Selesnick and Blake, 2000, and references therein). The convective transport is effective only for electrons with energies less than a few hundred keV. The energy gained from M -conserving radial transport can be significant, as is shown in Figure 4. The curves in this figure show how equatorially mirroring electrons that have the labeled energy at $L^* \sim 6.6$ gain energy as they are transported to lower L^* values. This is an ideal depiction and does not take into

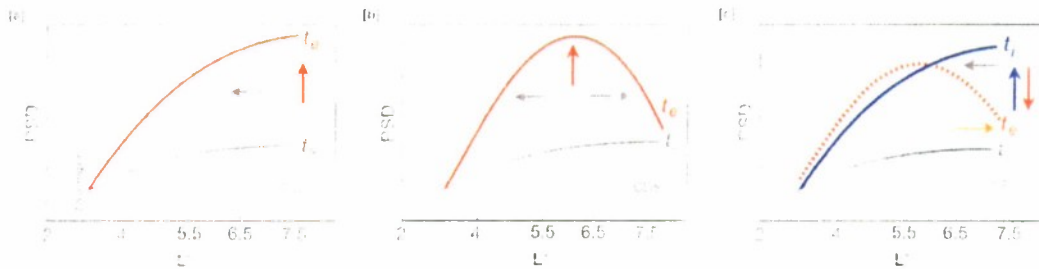


Figure 3. Cartoon showing examples of relativistic electron PSD radial profiles for different transport and acceleration assumptions. t_s represents the pre-storm profile and t_e the post-storm flux peak PSD profile. [a] Profile expected for pure inward radial transport (gray arrow) from large L^* source region of high PSD towards a smaller L^* region of lower PSD. [b] Profile from a combination of inward radial transport and internal acceleration with the latter resulting in a peak in PSD. [c] Profile that starts with inward radial transport from a region of high PSD at large L^* (blue arrow), but ends with outward radial transport (orange arrow) into a region of lower PSD at large L^* because of a delayed but dramatic PSD decrease at large L during storm recovery phase.

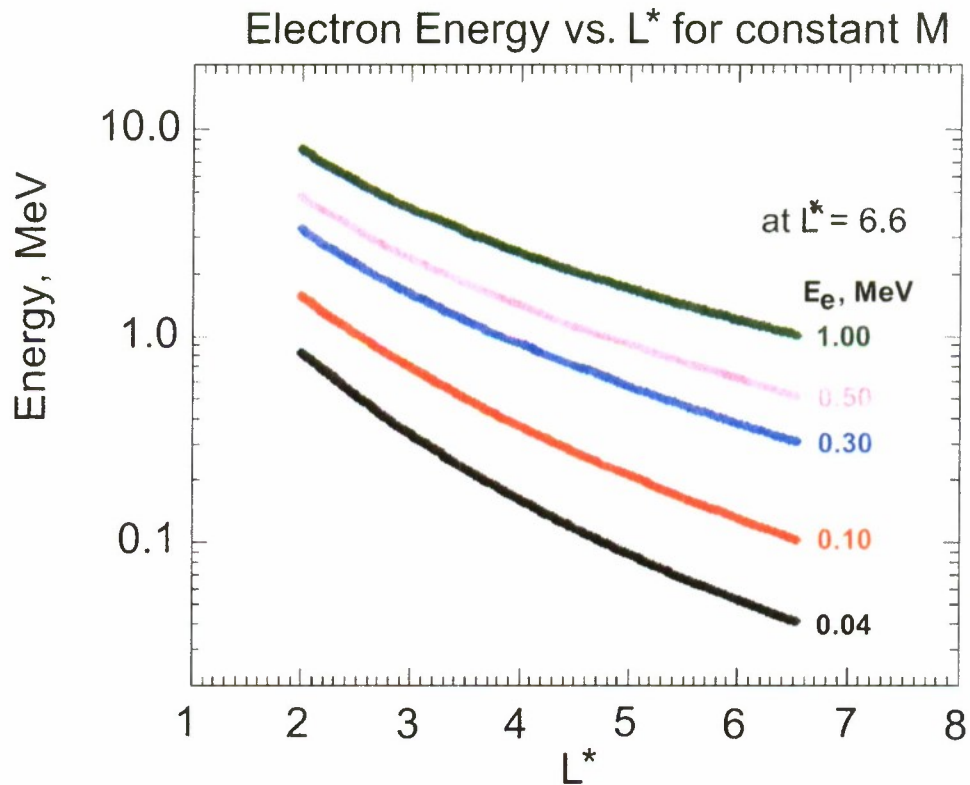


Figure 4. Energy gained by equatorially mirroring electrons starting near geosynchronous orbit as they are adiabatically transported to smaller L^* .

account the pitch angle dependence of the energy gain, the time frame required for the transport, nor whether sufficient wave power is present at the electron drift frequencies to support the transport to small L^* values. Such issues are discussed in the paper by O'Brien et al. (2003).

As noted above, the electron flux rise is observed to occur most rapidly at the L position that ultimately corresponds to the peak in the enhanced fluxes for MeV electrons. Tverskaya et al. (2003) showed that the L position of the post-storm MeV flux peak (L_{MAX}) could be organized in terms of the storm-time D_{ST} minimum. O'Brien and Moldwin (2003) showed that the plasmopause position, L_{PP} , was well correlated with D_{ST} . The Tverskaya et al. (2003) result was replotted by O'Brien et al. (2003) with the estimated plasmopause position from D_{ST} used to fit the L dependence of the flux peak. Those results are reproduced here as Figure 5. It shows that there is a strong correlation between the magnitude of a storm, as represented by D_{ST} , and the L value where the strongest enhancements in the MeV electron fluxes occur. O'Brien et al. (2003) and later Li et al. (2006) inferred that this relationship was the result of the erosion of the plasmopause, with the deepest penetration and position of maximum acceleration of the electrons occurring just outside the estimated eroded plasmasphere boundary, as indicated by the dashed L_{PP} curve in Figure 5. This is where it is expected that the VLF chorus is cutoff by the rising plasma density. So the picture that arises is one in which the source population is provided by convective and diffusive transport from large L^* , and those source particles are further energized by M breaking in the VLF chorus wave fields outside the plasmasphere. The source population contains the free energy that generates the waves and the particles to be energized. This is an example of the organization of the electron enhancements by the strength and penetration of substorm and storm-time electric fields during the main and early recovery phases of a magnetic storm.

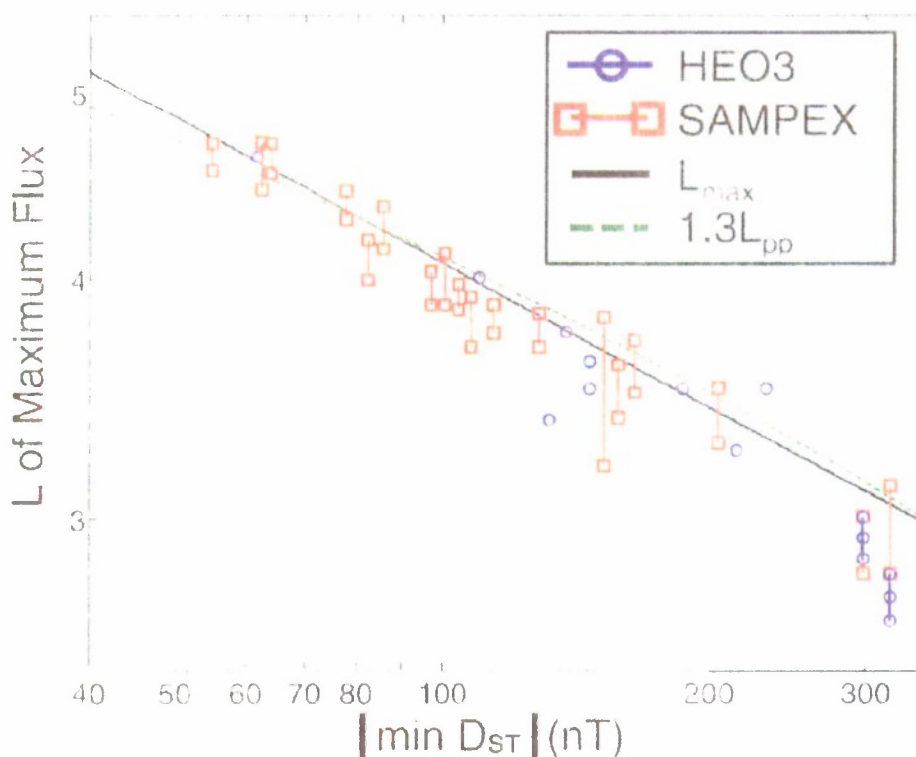


Figure 5. Location of the peak MeV electron fluxes as a function of storm minimum D_{ST} . The solid black curve is the L_{MAX} function from Tverskaya et al. (2003), and the dashed green curve is a scaled plasmopause position model L_{PP} from O'Brien and Moldwin (2003)

2.5 Source Populations

The source populations consist of the suprathermal electrons of the plasma sheet. It is thought that these electrons are brought into the inner magnetosphere, to geosynchronous and lower altitudes, from the near-Earth magnetotail by substorm injections and the storm-time convection that also brings the ring current ions into the inner magnetosphere (Baker et al., 2002; Blake et al., 2005; Jordanova, 2003. and references therein). The Blake et al. (2005) paper showed a linkage for the mid 10's to 100's keV electron fluxes between geosynchronous altitude and the Polar, Chandra, and Cluster satellite apogee altitudes (all well outside of geosynchronous) on the night side during one substorm. Other authors have shown similar results (e.g., Baker et al., 2002). There are still some questions about the relative timing of the arrival of such source or seed populations and the observed onsets of reconnection in the magnetotail.

An issue is whether the PSD in the plasma sheet is sufficient to provide the PSD gradient for classic diffusive transport to the inner magnetosphere. Li et al. (1997) had already determined that the solar wind electron PSD was not sufficient to account for the electron PSD in the inner magnetosphere via a radial transport process alone. However, those electrons would be a seed population for other processes that could increase their energy as they transitioned from the solar wind to the plasma sheet before being further transported to trapping regions of the inner magnetosphere. Polar and Cluster observations were used to investigate whether the plasma sheet source, exterior to the trapping regions, was a sufficient source to supply electrons to the inner magnetosphere by radial transport. Taylor et al. (2004) compared the PSD levels for electrons at the same M (0.6 MeV/G) at Cluster, Polar, geosynchronous, and GPS positions. They concluded that there did appear to be sufficient electron PSD in the plasma sheet out to 18 Re to support the classic diffusive transport process, but at the same time, they noted that the PSD was enhanced or peaked in the inner regions, and could not rule out the action of local acceleration mechanisms. They did note that the PSD levels measured at ~ 18 Re are highly dependent on where in the plasma sheet they are taken. The PSD values change quite dramatically from the plasma sheet boundary to the central plasma sheet and through the neutral sheet regions. Taylor et al. (2004) examined an interval of weak to moderate magnetic activity ($D_{ST} \geq -40$ nT), not representative of your typical magnetic storm. The question remains as to whether the plasma sheet PSD was high enough prior to large storms to supply the electrons for those events and whether the electrons measured at ~ 18 Re in the magnetotail are on closed drift trajectories. This issue of closed drift trajectories will be discussed in greater detail below.

There is some evidence by Shprits, et al. (2006) that the dramatic losses of electrons during the storm main phase could be partially caused by outward diffusion because of a dramatic drop in the PSD at high altitudes. They argue that the high pressure generated by the high-speed, high-density solar wind associated with magnetic storm onset brings the magnetopause boundary earthward. The low PSD exterior to the dayside boundary sets up the conditions for outward diffusion that lowers the PSD in the outer and inner regions of the magnetosphere for several hours. Other processes must then raise the PSD in the distant magnetosphere and magnetotail to supply the source populations for the ensuing PSD enhancements in the inner magnetosphere if radial transport is the dominant processes.

The M breaking processes would lead to a PSD radial profile different from that expected for pure diffusive transport. A possible example of this is shown in Figure, 3b and is much like the peak in the PSD radial profiles observed by Green and Kivelson (2004), Iles et al. (2006), Chen et al. (2007), and

Fennell and Roeder (2008). The PSD peak observed in the Polar HIST data by Green and Kivelson occurred at $L^* \sim 5$ at small equatorial pitch angles (large K values) for MeV electrons. The PSD peaks observed in the CRRES data by Iles et al. (2006) occurred for near equatorially mirroring \leq MeV electrons in the $L^* \sim 5-5.5$ region. Chen et al. (2007) used multiple satellite observations in a superposed epoch study covering two years of data and got a result that showed a peak in MeV electron ($M \sim 2.1$ MeV/G) PSD profile at near equatorial pitch angles for $L^* \sim 5.5$. Recently, Fennell and Roeder (2008) observed PSD peaks in near equatorially mirroring electrons, but at $<$ MeV energies. They did observe a peak in the \geq MeV electrons near $L^* \sim 5.5$, but only for electrons mirroring well off the equator. Near the equator, they observed a flat or negative slope in the radial profile for $4.7 < L^* < 7.5$. In fact, the PSD peak observed by Fennell and Roeder appears to be of the type shown in Figure 3c for the off-equatorial pitch angles. A summary PSD profile from Chen et al. (2007) is shown in Figure 6. In general, it shows a negative PSD gradient for $L^* \geq 6.5$ for storm main phase and for the recovery and average conditions. This would seem to be inconsistent with the results of Taylor et al. (2004) that indicated the plasma sheet PSD was consistent with that needed to support radial transport as a source of relativistic electrons. The PSD values at large L^* in Figure 6 would not support radial transport as a major mechanism for generating and maintaining the radiation belts, at least at the one M value Chen et al. (2007) studied. The differences between the limited observations indicate that further examination of this issue is needed.

Why would a peak form of the type shown in Figure 3c? This could occur if the electrons observed at large L^* are not on closed drift shells or the PSD dropped dramatically near the last closed drift shells during the storm recovery period. The use of the adiabatic invariants to organize the electrons and to remove the drift-shell splitting (Roederer, 1970) assumes that they move on closed drift trajectories.

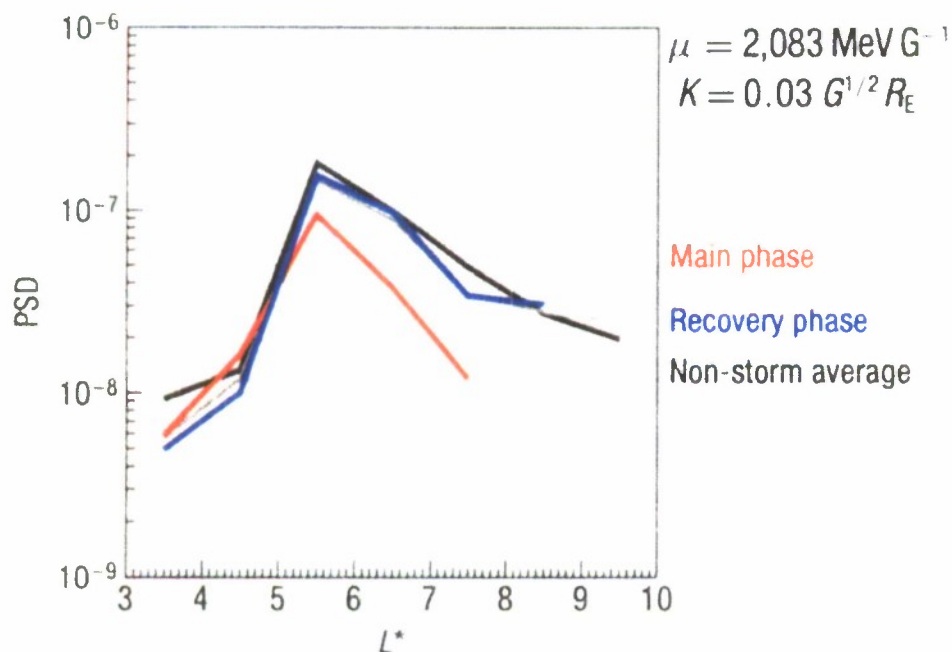


Figure 6. PSD radial profiles from Multisatellite observations during storm main and recovery phases plus comparisons to average PSD profiles. (after Chen et al. 2007).

Those on open drift trajectories violate the third adiabatic invariant and may violate conservation of the second and possibly even the first invariant in extreme cases. If the drift trajectories are open, one should not assume there is a linkage between the PSDs of electrons on those trajectories and those on closed drift trajectories. However, one does require that the electrons on open drift trajectories must be transported onto closed trajectories in order to provide a source for all processes that operate to reestablish and maintain the radiation belts. Fennell and Roeder (2008) observed that the off-equatorial mirroring electrons showed a strong gradient in PSD at higher L^* 's (≥ 6). In contrast, the simultaneously observed equatorially mirroring electrons had PSDs that were nearly constant for $L^* > 6.5$. An example from their paper, presented in Figure 7, shows this result. The model field (Tsyganenko et al., 2003; Tsyganenko and Sitnov, 2005) predicted that the electrons were on closed drift shells for both large and small K values, but the observations indicated that they most likely were not on closed drift shells at $K \sim 0.25$; otherwise, the PSD profiles should not have exhibited nearly order of magnitude drops within a narrow L^* region ($\Delta L^* < 0.5$ Re.) at the higher L^* 's. Fennell and Roeder (2008) did not observe such steep PSD gradients for equatorially mirroring electrons out to $L^* \sim 7.5$. However, it is not clear how far to larger L^* one could go along the magnetic equator and guarantee that the electrons are on closed drift trajectories. Based on the Fennell and Roeder (2008) observations, it is clear that magnetic field models may indicate that electrons are on closed drift shells when observations of very steep electron PSD gradients indicate that the drift shells are not closed.

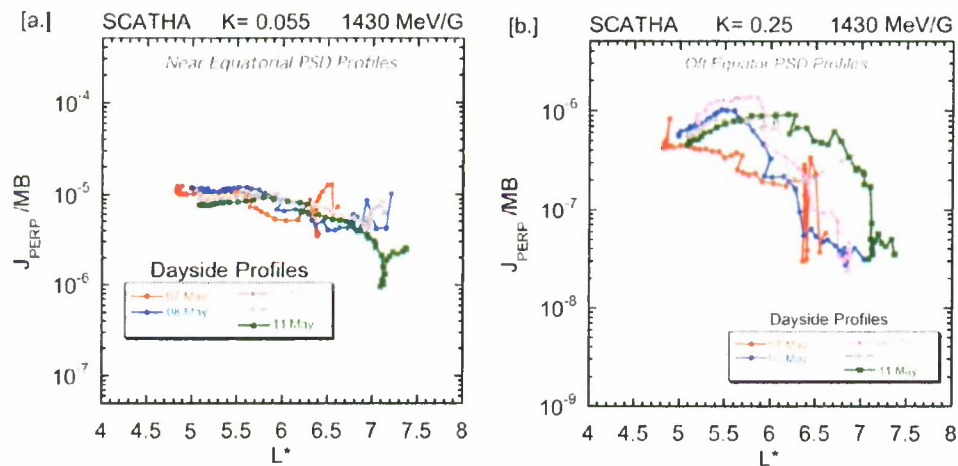


Figure 7. PSD radial profiles for small (panel [a]) and moderate K values (panel [b]). Note the difference in vertical scales for [a] and [b] (after Fennell and Roeder, 2008).

3. Energetic Electron Responses During July 2004 Storms

In the sections summarizing what we have learned, we did not provide an example of what a storm really looks like, beginning to end, from the perspective of satellites in the inner magnetosphere and plasma sheet. We do so here in an attempt to show the relationship between the near-Earth magnetotail electron fluxes and the changes deep in the inner magnetosphere, with emphasis on a moderately large storm. To do this, we use HEO3 and Cluster data from the period around 24 July 2004. For the HEO3 data, we extend the observations in the inner magnetosphere to include events that preceded and followed the 24 July storm by a few days. For Cluster, we focus on the early main phase portion of the July 24 storm.

3.1 Data Sources for Example Storms

HEO3 is a non-spinning satellite in a 12-hour, high-altitude, high-inclination orbit that crosses the same L and L^* values at two different MLT regions twice a day. The sensors on HEO3 measure the integral electron fluxes in six channels: E1 > 130 keV, E2 > 230 keV, E3 > 450 keV, E4 > 630 keV, E5 > 1.5 MeV, and E6 > 3 MeV. E4 to E6 are omni-directional sensors while E1-E2 and E3 are two telescopes. (Note: The HEO3 E1-E2 telescope temperature rose rapidly with altitude for the regions with $L \geq 5$ during the period of the study because of increased solar illumination as its attitude changed with altitude. The >130 and >230 keV electron channels became noisy as the temperatures rose. This raised their background levels, and limits their usefulness at large L .) The HEO3 trajectory is close to the magnetic equator from $L \sim 1.75$ to ~ 3 , but significantly far from it by $L \sim 6.5$ ($B/B_0 \sim 6.6$ in the Olson-Pfizer (1974, 1977) field model). For more details about HEO3, see Fennell et al., (2005).

The Cluster data is from the RAPID IES sensor (Wilken et al., 1997). IES measures electrons with energies of 40–400 keV in eight channels. It obtains 3D angular distributions in two broad energy channels. We will show the angular data for the 42–53 keV electrons. The data used here were taken when the Cluster spacecraft were traversing the plasma sheet near their apogee in the pre-midnight region on 24 July 2004.

3.2 HEO3 Observations of July 2004 Storms

There was a sequence of magnetic storm events starting late on July 16 with a -80 nT event, followed by events on July 22, 24, and 26 with D_{ST} minima of -101 nT, -148 nT, and -197 nT, respectively, as shown in Figure 8. Note that the D_{ST} minima were reached at 0300 UT on July 17, 0300 UT on July 23, 1200 UT on July 25, and 1400 UT on July 27. Examples of the electron responses in the inner magnetosphere are shown in Figure 9 using HEO3 data. Figure 9 shows the electron rates measured at nine different L and L^* values for the interval from 14 July to 8 August 2004. (L and L^* were obtained from the HEO3 magnetic ephemeris data base which was generated using the Olson-Pfizer field model.) Each panel is annotated with the L , L^* , and MLT where the data were taken,

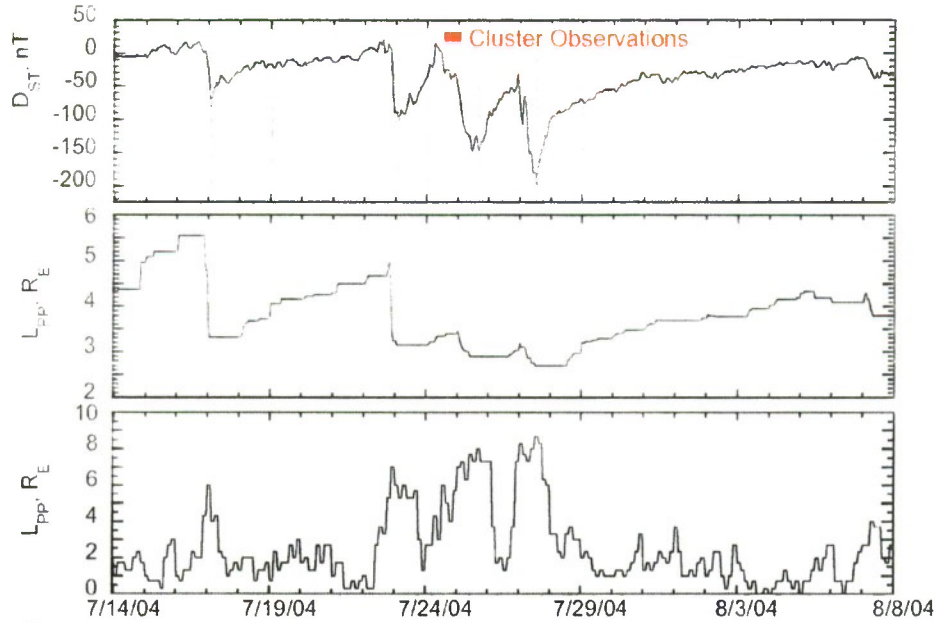


Figure 8. D_{ST} , L_{PP} , and K_p for the period 14 July to 8 August in 2004. The red bar indicates the period of the Cluster data used. The HEO3 data spanned the full time interval of the plots. L_{PP} is calculated from D_{ST} using the O'Brien and Moldwin (2003) formulation.

and the data from the individual energy channels are color-coded (see legends and caption for Figure 9). We binned the HEO3 data into L bins corresponding to $L = 1.75, 2.0, 2.25$, etc. up to $L = 10$, and show only a subset in Figure 9 to show the trends in the data. Figure 10 shows the solar wind parameters for only July 24. There was a sudden commencement-like positive excursion in D_{ST} prior to the main phase of the July 24 event, as seen in Figure 8. This was associated with the rotation in the interplanetary magnetic field and the solar wind speed jump near 1200 UT on July 24, as shown in Figure 10. The solar wind speed was above 550 km/s the whole day and, after the field rotation, the interplanetary field intensity was relatively constant for the remainder of the day.

We start by using the HEO3 data to examine the electron responses to magnetic activity preceding 24 July 2004 to see whether there are residual effects in the inner magnetosphere. The data in Figure 9 show that very deep in the inner magnetosphere at $L = 2$ ($L^* = 1.9$) the electron fluxes did not start rising until about 0000 UT on 25 July and then only in the lowest energy channels (see panel [a]). The 450- and 630-keV fluxes started rising near 0000 UT on 27 July, and the >1.5 MeV fluxes rose about a day later. At $L = 2$, there was not an electron response to the 16 and 22 July 2004 events, and there wasn't a response to any of the events in the >3 -MeV channel. The electrons with energies that would correspond to a "source" population were observed to rise about half way through the main phase of the 24 July event at $L = 2$. The higher energies did not start rising until ~ 48 h later during the secondary main phase that started late on 26 July. Thus, while there is evidence that "source" population electrons reached $L = 2$ during the 24 July event, there was not a corresponding increase in the relativistic electron population that deep in the inner magnetosphere.

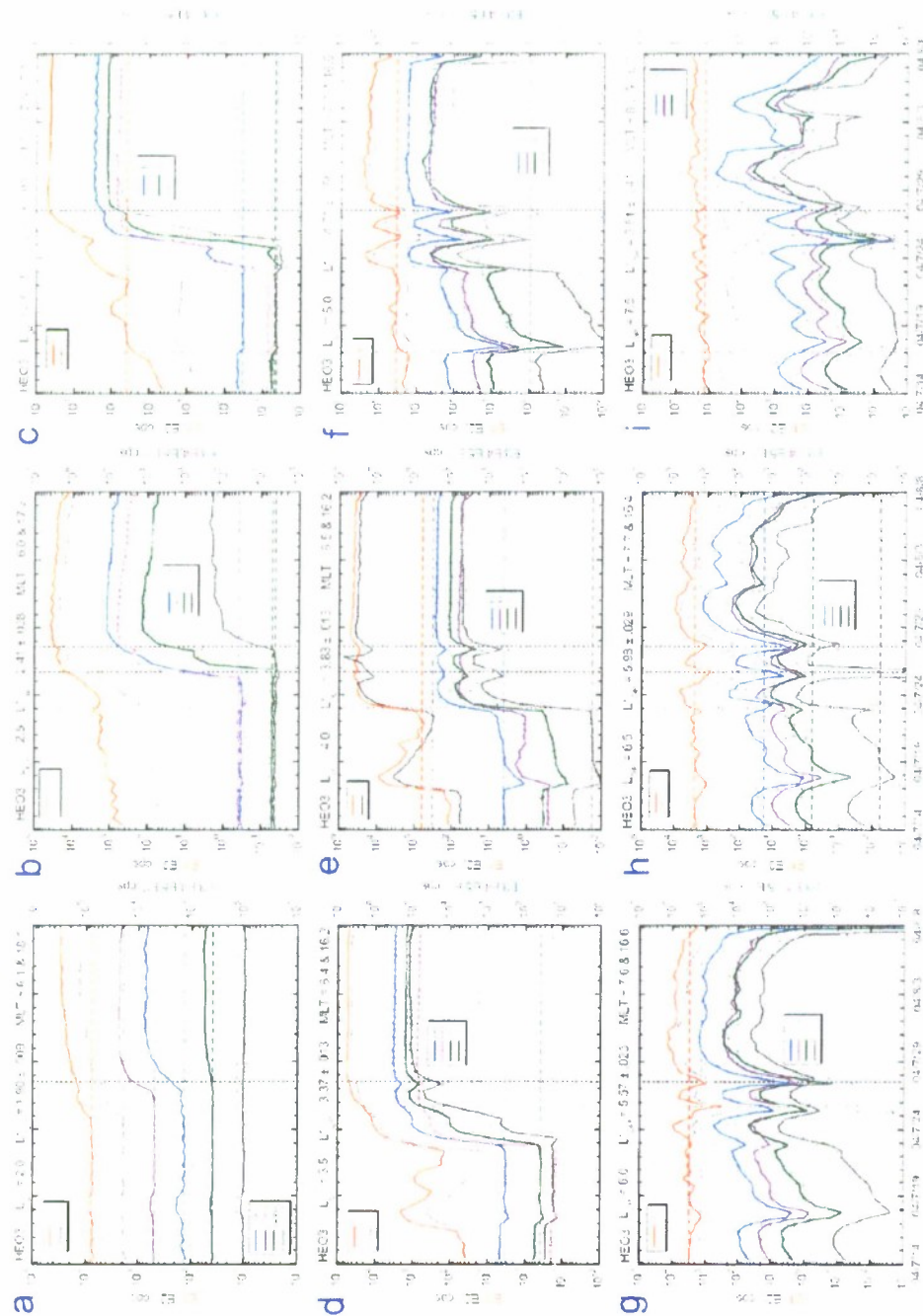


Figure 9. Coded electron intensity plots. The left- and right-hand vertical axes have different ranges for the channels indicated. Dashed vertical lines identify the time of the DST minimum for each event. The L, L*, and MLT are labeled at the top of each plot. The legends relate the colors to the electron energy channels with E1, E2, E3, E4, E5, E6, and E7 having energies >0.13 , >0.23 , >0.45 , >1.5 , and >3 MeV respectively.

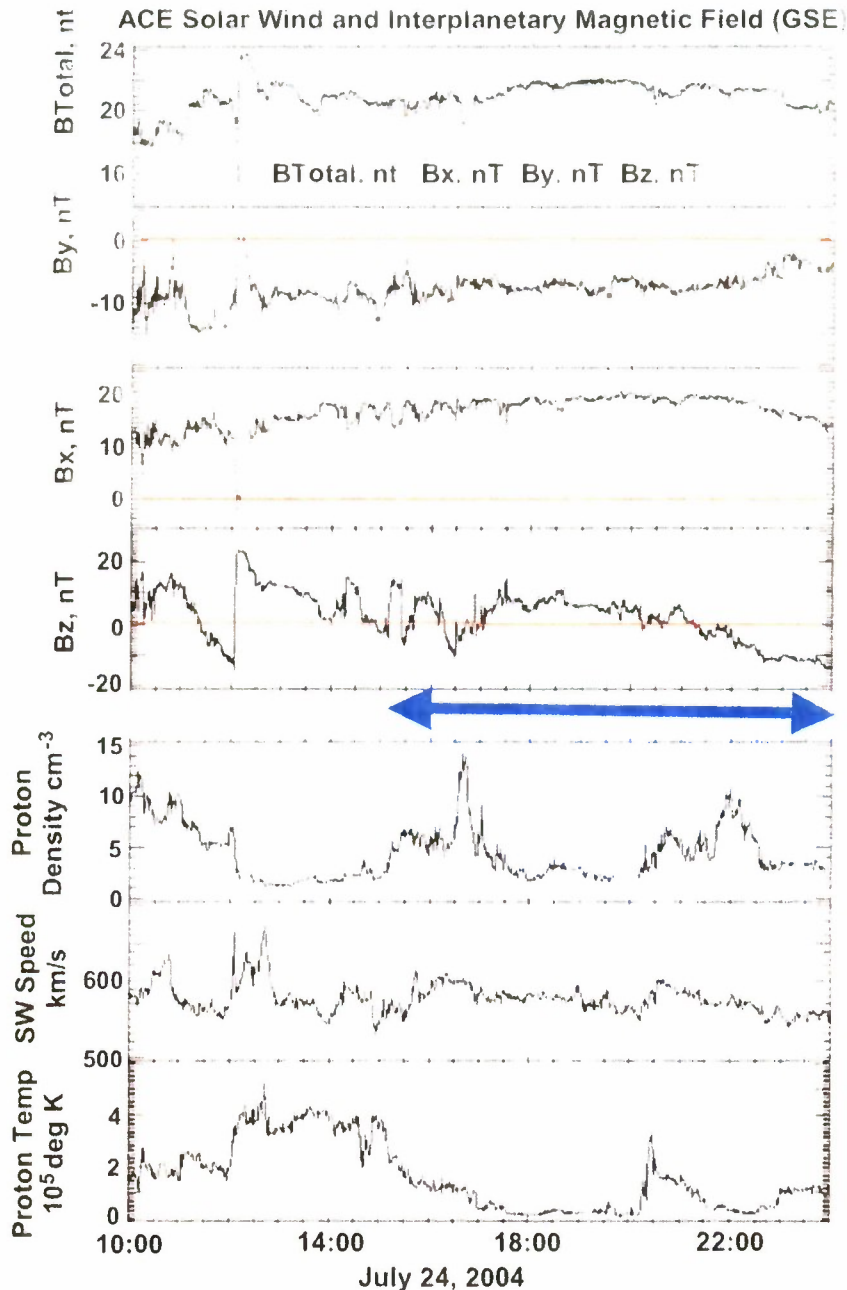


Figure 10. Interplanetary magnetic field (top four panels), solar wind density, speed, and proton temperature (bottom three panels) on July 24, 2004. The blue arrow marks the interval where the intense energetic plasma sheet electron fluxes were observed by Cluster.

At $L = 2.5$ ($L^* \sim 2.41$; see panel b), the electron responses to the 24 July event were significantly stronger than at $L = 2$. However, except for a gradual rise in the 130- and 230-keV electron fluxes over the 14–23 July interval, there was no clear higher energy electron response to the July 16 and 22 storms at $L = 2.5$. The 130- and 230-keV electron fluxes started a gradual rise near 0000 UT on July

24 that steepened near 1200 UT on 25 July. The 450- and 630-keV fluxes rose sharply near 1200 UT (i.e., near D_{ST} minimum) on 25 July at $L = 2.5$. The higher energy, >1.5 and >3 MeV, flux rises were more delayed, as is generally observed for all storm-time events, with the >3 -MeV fluxes starting to rise after 0800 UT on July 27 during the main phase of the July 26 storm. We note that the time history of the estimated L position of the plasma pause (L_{PP}) shown in Figure 8 had values $L_{PP} \geq 3.15$ for the July 16 and July 22 events, but had values of $L_{PP} = 2.9$ and 2.6 during the July 24 and July 26 events, respectively. [The L_{PP} values were obtained from D_{ST} using the O'Brien and Moldwin (2003) formulation.] The fact that relativistic electron fluxes were not observed at small L in response to the July 16 and July 22 storms may be consistent, if the L_{PP} values are accurate, with chorus waves not being present at these L values because they are inside the plasmapause boundary.

Separately, we note that if we used the L_{MAX} curve in Figure 4, we would expect the peak in the relativistic electron flux to be at $L \sim 4.3$ and ~ 4.1 for the July 16 and July 22 events respectively. Observationally, the peak fluxes occurred at $L \sim 4$ for the July 16 event at the four lowest energies, with no response at the two highest energies. The peak fluxes were at $L \sim 3.75$ – 4 at the three lowest energies, and at $L \sim 4.25$ for the three highest energies for the July 22 event. Similarly, the L_{MAX} curve in Figure 4 would indicate that the flux peaks for the July 24 and July 26 events should be at $L \sim 3.7$ and ~ 3.5 , respectively. The HEO3 data had the peak fluxes near $L \sim 3.5$ – 3.75 for the two lowest energies. It was difficult to tell for the July 24 event since near their peak values these lower energy electron fluxes only had a short plateau before they continued to rise in response to the July 26 event. They had well-defined temporal peaks at higher L values, but those were not the maximum fluxes. For July 24 and July 26 events, the higher energy channels (> 450 keV) had their peak fluxes near $L \sim 3.5$ for both events. At this L value, these higher energy fluxes were nearly constant for several days, following the July 26 event, after achieving their peak values (see Figure 9 panels [c]–[e]). The largest electron responses were to the July 24 and July 26 events. These events are only two days apart. At the highest L values, the July 26 event main phase caused a flux drop, so we are somewhat unsure of the peak flux from the July 24 event. We note that all the available L values, not just those in Figure 9, were used in searching for the L of maximum flux for each event.

At L values from 3.0 to 6.5, the fluxes were observed to rise on 23 July, and reached an initial peak or a plateau early on 24 July, and then further increased on 25 July or fell, depending on the L value. The main response to the July 16 event was a flux drop for >450 keV electrons at all L s, and a rise in the 130 and 230 keV “source” electron fluxes only at $L = 3.0$ – 4.0 RE (Figure 9, panels [c] to [e]). (The HEO3 low-energy telescope temperature rose rapidly with altitude for the regions with $L \geq 5$ because of increased solar illumination. The 130- and 230-keV electron channels started getting noisy, and their background levels rose. The E1 channel was unusable and was deleted from panels [g]–[i] in Figure 9, while the E2 channel has a high background for those L values. Thus, our measurements of the source electron fluxes are uncertain for $L \geq 4.5$.)

3.3 Cluster Observations of July 24, 2004 Storm

As noted above, the July 24 event caused a strong response in electrons deep in the inner magnetosphere. During the interval 24–26 July, the solar wind speed was enhanced, and IMF B_z turned southward starting at ~ 2100 on July 24 (see Figure 10), reaching a level of ~ -20 nT early on July 25, and remained at that level until ~ 1520 UT that day (not shown). Cluster transitioned from the near-Earth tail-lobe, boundary layer and plasma sheet region prior to and during the main phase of this

event, as evidenced by the IES electron fluxes in Figure 11. The spin average energetic electron fluxes were very similar at all four Cluster spacecraft throughout July 24. The spacecraft were in the magnetotail on the morning side, near 3 MLT, during the onset of a -148 nT storm that started gradually near 1200 UT (ref Figure 8). At the time of the storm onset, the Cluster spacecraft appeared to be in the tail lobe or near the high-latitude boundary of the plasma sheet, as evidenced by the lack of electron fluxes observed by the IES sensor on all four cluster satellites in Figure 11 and the weak ion fluxes observed by CIS (not shown).

As the main phase of the July 24 storm progressed a bit, the Los Alamos geosynchronous satellites near midnight observed a substorm injection around 1300 UT (not shown). The Los Alamos satellites also observed a second injection near 2320 UT, but none in between. The Cluster spacecraft entered the plasma sheet about three hours later, just before 1600 UT, while the $D_{ST} \sim -30$ nT and K_p was falling from +6 to +5. The steepest decline in D_{ST} occurred after ~ 2200 UT on July 24. Between

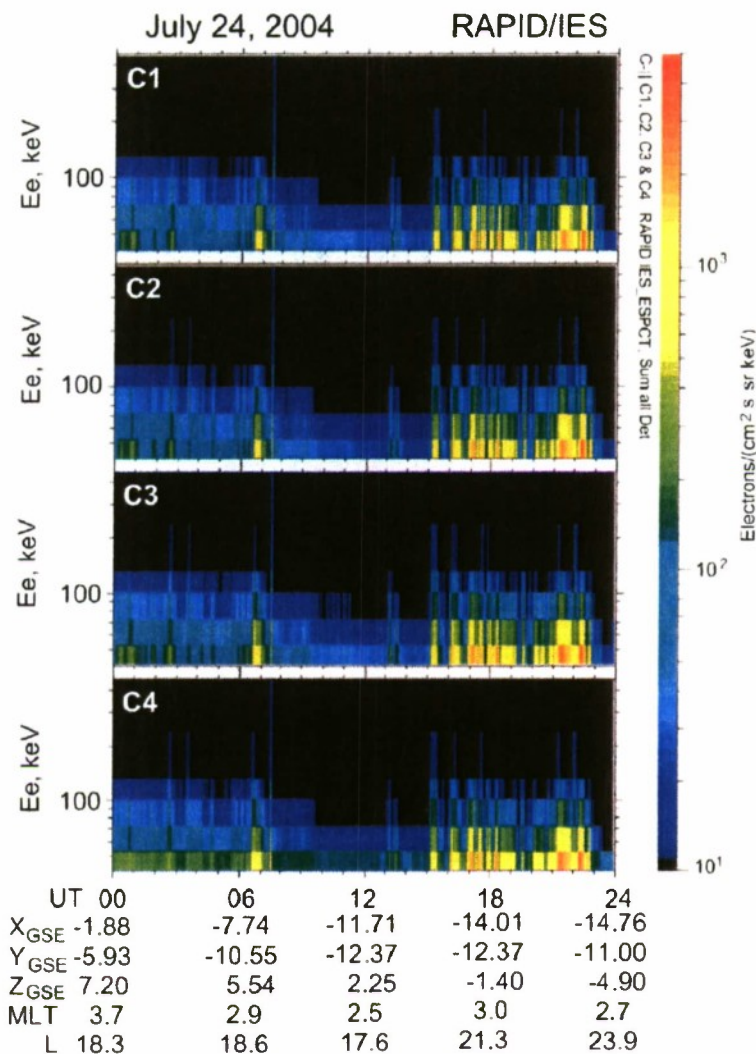


Figure 11. Spectrograms of spin-averaged electron fluxes measured by RAPID/IES on all four Cluster spacecraft for 24 July 2004.

1700 and 2400 UT, the Cluster IES instruments observed intense fluxes of field-aligned electron (FAE) distributions as shown in Figure 12. These FAE distributions were not constant, but occurred whenever Cluster entered the plasma sheet during this interval, as indicated by the FGM (Balogh et al. 1979) B_x and B_T measurements in Figure 12a. These FAE fluxes, with pitch angles $<30^\circ$, mirror closer to the Earth where the field intensity is more than twice that at Cluster. The electron distributions observed at Cluster can convect inwards in the storm time electric field to become the source population for the subsequent enhancements observed by the HEO3 spacecraft. The energetic elec-

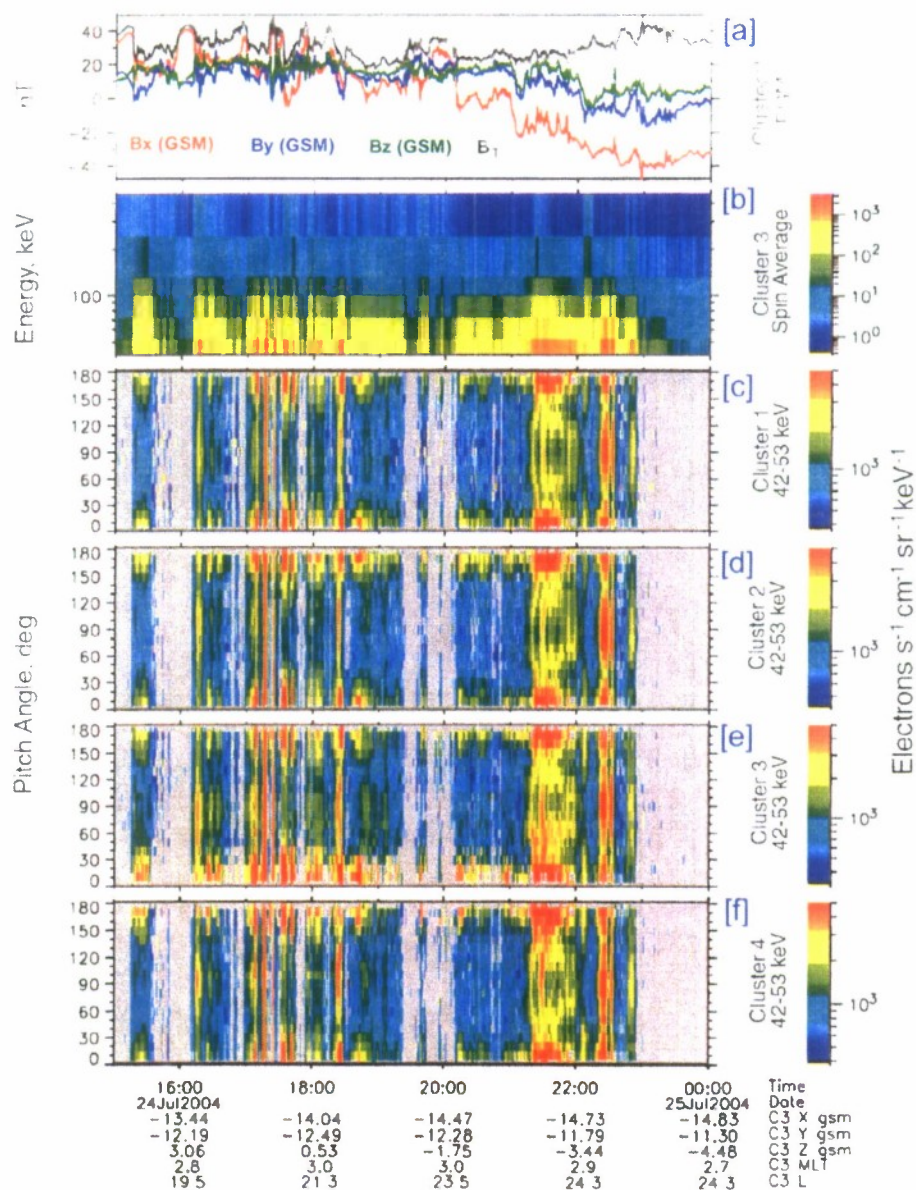


Figure 12. Cluster 3 magnetic field measurements (top panel), energy-time spectrogram of RAPID IES spin averaged fluxes on C3 (second panel), and RAPID IES angular distributions from all four Cluster spacecraft (bottom four panels) for the interval 1530-2400 UT on 24 July 2004.

trons observed at Cluster are not purely field aligned. The fluxes at 90° pitch angle were at times comparable to or $\sim 50\%$ of the FAE fluxes. In general, early in the storm main phase, Cluster observed about an order of magnitude increase in the 40–400 keV plasma sheet electron fluxes from those prior to the main phase onset as shown in Figure 11.

The long duration of energetic FAE is unique and not understood at this time. The existing models of magnetotail processes can support FAE from reconnection for a matter of minutes, but not for very extended periods and certainly not for hours. The fact that they are present every time Cluster reentered the plasma sheet of the ~ 6 -hour period shown in Figure 12 requires that either they were present continuously in the plasma sheet for that long of a period or that there were at least seven or more reconnection events in that period. The period 2020 to 2300 UT in Figure 12 shows that FAE were present essentially that whole time. This cannot be explained by the standard models. These 24 July FAE fluxes can be contrasted to those observed by Åsnes et al. (2008) and Taylor et al. (2006), both of which were very short in duration and consistent with expectations for a reconnection event.

Cluster left the plasma sheet and entered the tail lobe prior to the substorm onset observed by the Los Alamos satellites near 2320 UT on July 24. It did not reenter the plasma sheet until about 0030 UT on July 25. At that time, the energetic electron fluxes observed by IES had returned to normal pre-storm levels (not shown). Enhanced levels of energetic electron fluxes were not observed again at Cluster until after 0250 UT on July 25, and they were still at levels lower than those observed prior to 2300 UT on July 24. It is not until ~ 0630 UT on July 25 that Cluster observed energetic electron flux levels comparable to those observed in Figure 10, and then for less than an hour. Cluster spent most of the rest of July 25 in the tail lobe, with occasional intervals in the boundary layer and very short intervals in plasma sheet like plasma. During this period, D_{ST} reached its minimum of -148 nT at 1000 UT, and the recovery period started.

As Figure 9 shows, by mid day on 25 July the energetic electron enhancements deep in the inner magnetosphere (see Figures 9 a and b) were well under way. The source fluxes (130- and 230-keV fluxes) that were transported deep into the inner magnetosphere initially arrived at low L late on July 24 and early on July 25. We cannot tell exactly when from the HEO3 observations because of sparse sampling due to its 12-hour orbital period. It is clear from Figure 9 that the >450 -keV electrons had reached low L values by the time of or just after D_{ST} minimum. The sequence is less clear for $L \geq 3$ because of the preexisting enhanced >100 keV fluxes that remained from the earlier activity. However, the >3 MeV fluxes are definitely rising by ~ 1200 UT on July 25 at $L = 3$. So not only are the source type electrons present by the time of early recovery, but also the accelerated or high-energy fluxes. The fact that the intense 40–400 keV electron fluxes were observed at Cluster during the early storm main phase, very late on July 24, combined with the clear rise of fluxes of electrons at low L with energies consistent with those observed in the plasma sheet (but raised in energy by transport as in Figure 5) provides strong circumstantial evidence that the electrons observed by Cluster are very possibly the source for the subsequent enhancements of MeV fluxes deep in the inner magnetosphere.

4. Summary

Examination of historical and current results that describe and attempt to understand what causes the enhancements of electron fluxes in the inner magnetosphere's radiation belts has narrowed the current research focus onto basically two mechanisms. Radial transport from the near-Earth plasma sheet while conserving the particle's magnetic moment has been considered the primary mechanism for a long time. More recently, in the last decade, mechanisms that break conservation of M have been strongly considered. Much of the recent observational evidence points to the necessity for M -breaking mechanisms in localized regions, for example $5 \leq L^* \leq 6$, if one is to explain PSD peaks there even if radial transport is also operating. However, the discussion is not closed because there is conflicting evidence, and the number of observational studies is still relatively small. The Cluster and HEO3 storm response example shown above hints that transport could explain the rapid appearance of particles to near 0.5 MeV energies at very low L values prior to or at D_{ST} minimum during some storms. This provides a reason to continue to look carefully at the processes and to try to find ways to test the different models. However, one major difficulty that we currently have to contend with is that it usually takes multiple observation platforms to obtain the necessary physical space and energy sampling to trace the PSD from the distant plasma sheet to low L values in the magnetosphere. This requires very careful intercalibration of disparate datasets. In addition, except for the CRRES observations (Meredith et al., 2002a, 2002b, 2003), there are not simultaneous wave measurements that can be used to assess whether the M -breaking mechanisms are operating or not in most of the recent studies. It is hoped that the NASA RBSP mission will help solve some of this difficulty because it covers the whole inner magnetosphere with electron instruments that have a wide range, covering plasma-sheet to highly relativistic energies, has the wave and field measurements needed, and with its two platforms, will increase the sampling cadence for determining the L dependence of the PSD profiles. However the RBSP must still rely on a second set of measurements within the distant plasma sheet.

References

- Åsnes, A., M. G. G. T. Taylor, A. L. Borg, B. Lavraud, R. W. H. Friedel, C. P. Escoubet, H. Laakso, I. Daly, and A. N. Fazakerley, Multispacecraft observation of electron beam in reconnection region, *J. Geophys. Res.*, **113**, A07S30, doi:10.1029/2007JA012770, 2008.
- Baker D. N., W. K. Peterson, S. Eriksson, X. Li, J. B. Blake, J. L. Burch, P. W. Daly, M. W. Dunlop, A. Korth, E. Donovan, R. Friedel, T. A. Fritz, H. U. Frey, S. B. Mende, J. Roeder, and H. J. Singer, "Timing of magnetic reconnection initiation during a global magnetospheric substorm onset," *Geophys Res Lett*, **29**, 2190, doi:10.1029/2002GL015539, 2002.
- Balogh, A., M. W. Dunlop, S. W. H. Cowley, et al., "The Cluster magnetic fields investigation," *Space Sci. Rev.* **79**, 65, 1997.
- Blake J. B., R. Mueller-Mellin, J. A. Davies, X. Li, and D. N. Baker, "Global observations of energetic electrons around the time of a substorm on 27 August 2001," *J Geophys Res*, **110** A06214, doi:10.1029/2004JA010971, 2005.
- Blake J. B., R. S. Selesnick, D. N. Baker, and S. Kanekal, "Studies of relativistic electron injection events in 1997 and 1998," *J Geophys Res*, **106**, 19157, 2001.
- Blake, J. B., D. N. Baker, N. Turner, K. W. Ogilvie, and R. P. Lepping, "Correlation of changes in the outer-zone relativistic-electron population with upstream solar wind and magnetic field measurements," *Geophys Res. Lett*, **24**, 927, 1997.
- Bortnik, J. and R. M. Thorne, "The dual role of ELF/VLF chorus waves in the acceleration and precipitation of radiation belt electrons," *JSAPT*, **69**, 378, doi:10.1016/j.jastp.2006.05.030, 2007.
- Chen Y., G. Reeves, R. H. W. Friedel, "The energization of relativistic electrons in the outer Van Allen radiation belt," *Nature Physics*, **3**, 614, 2007.
- Elkington, S. R., M. K. Hudson, and A. A. Chan, "Acceleration of relativistic electrons via drift-resonant interaction with toroidal-mode Pc-5 ULF oscillation," *Geophys Res Lett*, **26**, 3273, 1999.
- Elkington, S. R., M. K. Hudson, and A. A. Chan, "Resonant acceleration and diffusion of outer zone electrons in an asymmetric geomagnetic field," *J. Geophys. Res.*, **108**, (A3), 1116, doi:10.1029/2001JA009202, 2003
- Falthammer, C. G., "Radial diffusion by violation of the third adiabatic invariant," *Earths Particles and Fields*. Reinhold, New York, p. 157, 1968.
- Fennell, J. F. and J. L. Roeder, "Storm time phase space density radial profiles of energetic electrons for small and large K values: SCATHA results," *Journal of Atmospheric and Solar-Terrestrial Physics*, doi:10.1016/j.jastp.2008.03.014, 2008.

- Fennell, J. F., J. B. Blake, R. Friedel, and S. Kanekal, "The Energetic Electron Response to Magnetic Storms: HEO Satellite Observations, in Physics and Modeling of the Inner Magnetosphere." *AGU monograph* **155**, p. 87, 2005.
- Friedel, R. H. W., G. D. Reeves, and T. Obara, "Relativistic electron dynamics in the inner magnetosphere—a review," *J. Atmospheric and Solar Terrestrial Physics*, **64**, 265, 2002.
- Fujimoto, M., and A. Nishida, "Energization and anisotropization of energetic electrons in the Earth's radiation belt by the recirculation process," *J Geophys Res*, **95**, 4265, 1990.
- Green, J. C., and M. G. Kivelson, "Relativistic electrons in the outer radiation belt: differentiating between acceleration mechanisms," *J. Geophys Res*, **109**, doi:10.1029/2003JA010153, 2004.
- Green, J. C., T. G. Onsager, T. P. O'Brien, and D. N. Baker, "Testing loss mechanisms capable of rapidly depleting relativistic electron flux in the Earth's outer radiation belt," *J. Geophys Res*, **109**, A1224, 2004.
- Horne, R. B., N. P. Meredith, R. M. Thorne, D. Heynderickx, R. H. A. Iles, and R. R. Anderson, "Evolution of energetic electron pitch angle distributions during storm time electron acceleration to megaelectronvolt energies," *J. Geophys Res*, **108**, 1016, doi:10.1029/2001JA009165, 2003.
- Horne, R., R. M. Thorne, S. A. Glauert, J. M. Albert, N. P. Meredith, and R. R. Anderson, "Timescale for radiation belt electron acceleration by whistler mode chorus waves," *J Geophys Res*, **110**, A03225, doi:10.1029/2004JA010811, 2005.
- Horne, R., R. M. Thorne, S. A. Glauert, N. P. Meredith, D. Pokhotelov, and O. Santolík, "Electron acceleration in the Van Allen radiation belts by fast magnetosonic waves," *Geophys. Res. Lett.*, **34**, L17107, doi:10.1029/2007GL030267, 2007,
- Hudson, M. K., S. R. Elkington, J. G. Lyon, M. J. Wiltberger, and M. Lessard, "Radiation belt electron acceleration by ULF wave drift resonance: Simulation of 1997 and 1998 storms," *Space Weather*, **125**, edited by P. Song, H. J. Singer, and G. L. Siscoe, p. 289, AGU, Washington, D. C., 2001.
- Hudson, M. K., S. R. Elkington, J. G. Lyon, V. A. Marchenko, I. Roth, M. Temerin, J. B. Blake, M. S. Gussenhoven, J. R. Wygant, "Simulations of radiation belt formation during storm sudden commencements," *J. Geophys Res*, **102**, 14087, 1997.
- Iles, R. H. A., N. P. Meredith, A. N. Fazakerley, and R. B. Horne, "Phase space density analysis of the outer radiation belt energetic electron dynamics," *J. Geophys Res*, **111**, A03204, doi:10.1029/2005JA011206, 2006.
- Jordanova, V. K., "New insights on geomagnetic storms from model simulations using multi-spacecraft data," *Sp. Sci. Rev.*, **107**, 157, 2003.
- Kaufmann, R. L., "Conservation of the first and second adiabatic invariants," *J. Geophys Res*, **70**, 2181, 1965.

- Li, X., D. N. Baker, T. P. O'Brien, L. Xie, and Q. G. Zong, "Correlation between the inner edge of outer radiation belt electrons and the innermost plasmapause location," *Geophys. Res. Lett.*, **33**, L14107, doi:10.1029/2006GL026294, 2006.
- Li, X., I. Roth, M. Temerin, J. R. Wygant, M. K. Hudson, and J. B. Blake, "Simulations of the prompt energization and transport of radiation belt particles during the March 24, 1991 SSC," *Geophys. Res. Lett.*, **20**, 2423, 1993.
- Lorentzen, K. R., J. B. Blake, U. S. Inan, and J. Bortnik, "Observations of relativistic electron microbursts in association with vlf chorus," *J. Geophys. Res.*, **106**, 6017, 2001.
- Lorentzen, K. R., J. E. Mazur, M. E. Looper, J. F. Fennell, and J. B. Blake, "Multisatellite observations of MeV ion injections during storms," *J. Geophys. Res.*, **107**, 1231, 2002.
- McAdams, K. L. and G. D. Reeves, "Non-adiabatic relativistic electron response," *Geophys. Res. Lett.*, **28**, 1879–1882, 2001.
- McIlwain, C. E., "Coordinates for Mapping the Distribution of Magnetically Trapped Particles," *J. Geophys. Res.*, **66**, 3681, 1961.
- Meredith, N. P., R. B. Horne, D. Summers, R. M. Thorne, R. H. A. Iles, D. Heynderickx, and R. R. Anderson, "Evidence for acceleration of outer zone electrons to relativistic energies by whistler mode chorus," *Ann. Geophys.* **20**, 967, 2002b.
- Meredith, N. P., R. B. Horne, R. H. A. Iles, R. M. Thorne, D. Heynderickx, and R. R. Anderson, "Outer zone relativistic electron acceleration associated with substorm-enhanced whistler mode chorus," *J. Geophys. Res.*, **107**, doi:10.1029/2001JA900146, 2002a.
- Meredith, N., R. B. Horne, S. A. Glauert, R. M. Thorne, D. Summers, J. M. Albert, and R. R. Anderson, "Energetic outer zone electron loss timescales during low geomagnetic activity," *J. Geophys. Res.*, **111**, A05212, doi:10.1029/2005JA011516, 2006.
- Meredith, N., R. M. Thorne, R. B. Horne, D. Summers, B. J. Fraser, and R. R. Anderson, "Statistical analysis of relativistic electron energies for cyclotron resonance with EMIC waves observed on CRRES," *J. Geophys. Res.*, **108**, 1250, doi:10.1029/2002JA009700, 2003.
- O'Brien, T. P. and M. B. Moldwin, "Empirical plasmapause models from geomagnetic indices," *Geophys. Res. Lett.* **30**, 1152, 2003.
- O'Brien, T. P., K. R. Lorentzen, I. R. Mann, N. P. Meredith, J. B. Blake, J. F. Fennell, M. D. Looper, D. K. Milling, and R. R. Anderson, "Energization of relativistic electrons in the presence of ULF power and MeV microbursts: Evidence for dual ULF and VLF acceleration," *J. Geophys. Res.*, **108**, 1329, doi:10.1029/2002JA009784, 2003.
- Olson, W. P. and K. A. Pfitzer, "A Quantitative Model of the Magnetospheric Magnetic Field," *J. Geophys. Res.*, **79**, 3739, 1974.
- Olson, W. P. and K. A. Pfitzer, "Magnetospheric magnetic field modeling," Annual Scientific Report, AFOSR Contract No. F44620-75-C-0033, 1977.

- Onsager, T. G., G. Rostoker, H.-J. Kim, G. D. Reeves, T. Obara, H. J. Singer, and C. Smithtro, "Radiation belt electron flux dropouts: Local time, radial, and particle-energy dependence," *J. Geophys. Res.*, **107**, 1382, doi:10.1029/2001JA000187, 2002.
- Paulikas, G. A. and J. B. Blake, "Effects of the solar wind on magnetospheric dynamics: Energetic electrons at the synchronous orbit," *Quantitative Modeling of Magnetospheric Processes*, p. 180, WP Olsen, ed., Am. Geophys. Union, Washington, D C. 1975
- Roederer, J. G., *Dynamics of geomagnetically trapped radiation*, Springer Verlag, Heidelberg-New York, 1970.
- Schulz, M. and L. J. Lanzerotti, Physics and Chemistry in Space, vol. 7, *Particle Diffusion in the Radiation Belts*, Springer-Verlag, New York, 1974.
- Selesnick, R. S., "Source and loss rates of radiation belt relativistic electrons during magnetic storms," *J. Geophys. Res.*, **111**, A04210, doi:10.1029/2005JA011473, 2006.
- Selesnick, R. S. and J. B. Blake, "On the source location of radiation belt relativistic electrons," *J. Geophys. Res.*, **105**, 2607, 2000.
- Shprits, Y. Y. and R. M. Thorne, "Time dependent radial diffusion modeling of relativistic electrons with realistic loss rates," *Geophys. Res. Lett.*, **31**, L08805, doi:10.1029/2004GL019591, 2004.
- Shprits, Y. Y., R. M. Thorne, R. B. Horne, S. A. Glauert, M. Cartwright, C. T. Russell, D. N. Baker, and S. G. Kanekal, "Acceleration mechanism responsible for the formation of the new radiation belt during the 2003 Halloween solar storm," *Geophys. Res. Lett.*, **33**, L05104, doi:10.1029/2005GL024256, 2006.
- Shprits, Y. Y., R. M. Thorne, R. Friedel, G. D. Reeves, J. Fennell, D. N. Baker, and S. G. Kanekal, "Outward radial diffusion driven by losses at magnetopause," *J. Geophys. Res.*, **111**, A11214, doi:10.1029/2006JA011657, 2006.
- Summers, Danny and Chun-yu Ma, "Rapid acceleration of electrons in the magnetosphere by fast-mode MHD waves," *J. Geophys. Res.*, **105**, 15,887-15,895, 2000.
- Taylor, M. G. G. T., R. H. W. Friedel, G. D. Reeves, M. W. Dunlop, T. A. Fritz, P. W. Daly, and A. Balogh, "Multisatellite measurements of electron phase space density gradients in the Earth's inner and outer magnetosphere," *J. Geophys. Res.*, **109**, A05220, doi:10.1029/2003JA010294, 2004.
- Taylor, M. G. G. T., G. D. Reeves, R. H. W. Friedel, M. F. Thomsen, R. C. Elphic, J. A. Davies, M. W. Dunlop, H. Laakso, B. Lavraud, D. N. Baker, J. A. Slavin, C. H. Perry, C. P. Escoubet, A. Masson, H. J. Opgenoorth, C. Vallat, P. W. Daly, A. N. Fazakerley, and E. A. Lucek, "Cluster encounter with an energetic electron beam during a substorm," *J. Geophys. Res.*, **111**, A11203, doi:10.1029/2006JA011666, 2006.
- Thorne, R. M., T. P. O'Brien, Y. Y. Shprits, D. Summers, and R. B. Horne, "Timescale for MeV electron microburst loss during geomagnetic storms," *J. Geophys. Res.*, **110**, A09202, doi:10.1029/2004JA010882, 2005.

- Thorne, R. M., Y. Y. Shprits, N. P. Meredith, R. B. Horne, W. Li, and L. R. Lyons, "Refilling of the slot region between the inner and outer electron radiation belts during geomagnetic storms," *J. Geophys. Res.*, **112**, A06203, doi:10.1029/2006JA012176, 2007.
- Tsyganenko, N. A. and M. I. Sitnov, "Modeling the dynamics of the inner magnetosphere during strong geomagnetic storms," *J. Geophys. Res.*, **110**, A03208, doi:10.1029/2004JA010798, 2005.
- Tsyganenko, N. A., H. J. Singer, and J. C. Kasper, "Storm-time distortion of the inner magnetosphere: How severe can it get?," *J. Geophys. Res.*, **108**(A5), 1029, doi:10.1029/2002JA009808, 2003.
- Tverskaya, L. V., N. N. Pavlov, J. B. Blake, R. S. Selesnick, and J. F. Fennell, "Predicting the L-position of the storm-injected relativistic electron belt," *Adv Space Res*, **31**, 1039, 2003.
- Wilken, B., W. I. Axford, I. Daglis, P. Daly, W. Güttler, W. H. Ip, A. Korth, G. Kremser, S. Livi, V. M. Vasiliunas, J. Woch, D. N. Baker, R. D. Belian, J. B. Blake, J. F. Fennell, L. R. Lyons, H. Borg, T. A. Fritz, F. Gliem, R. Rathje, M. Grande, D. Hall, K. Kecskemety, S. McKenna-Lawlor, K. Mursula, Tanskanen, Z. Pu, I. Sandahl, E. T. Sarris, M. Scholer, M. Schulz, F. Sorass, and S. Ullaland, "RAPID: The Imaging Energetic Particle Spectrometer on Cluster," *Space Sci. Rev.*, **79**, 399–473, 1997.
- Young, S. L., R. E. Denton, B. J. Anderson, and M. K. Hudson, "Empirical model for μ scattering caused by field line curvature in a realistic magnetosphere," *J. Geophys. Res.*, **107**, 1069, doi:10.1029/2000JA000294, 2002.
- Young, S. L., R. E. Denton, B. J. Anderson, and M. K. Hudson, "Magnetic field line curvature induced pitch angle diffusion in the inner magnetosphere," *J. Geophys. Res.*, **113**, A03210, doi:10.1029/2006JA012133, 2008.

PHYSICAL SCIENCES LABORATORIES

The Aerospace Corporation functions as an "architect-engineer" for national security programs, specializing in advanced military space systems. The Corporation's Physical Sciences Laboratories support the effective and timely development and operation of national security systems through scientific research and the application of advanced technology. Vital to the success of the Corporation is the technical staff's wide-ranging expertise and its ability to stay abreast of new technological developments and program support issues associated with rapidly evolving space systems. Contributing capabilities are provided by these individual organizations:

Electronics and Photonics Laboratory: Microelectronics, VLSI reliability, failure analysis, solid-state device physics, compound semiconductors, radiation effects, infrared and CCD detector devices, data storage and display technologies; lasers and electro-optics, solid-state laser design, micro-optics, optical communications, and fiber-optic sensors; atomic frequency standards, applied laser spectroscopy, laser chemistry, atmospheric propagation and beam control, LIDAR/LADAR remote sensing; solar cell and array testing and evaluation, battery electrochemistry, battery testing and evaluation.

Space Materials Laboratory: Evaluation and characterizations of new materials and processing techniques: metals, alloys, ceramics, polymers, thin films, and composites; development of advanced deposition processes; nondestructive evaluation, component failure analysis and reliability; structural mechanics, fracture mechanics, and stress corrosion; analysis and evaluation of materials at cryogenic and elevated temperatures; launch vehicle fluid mechanics, heat transfer and flight dynamics; aerothermodynamics; chemical and electric propulsion; environmental chemistry; combustion processes; space environment effects on materials, hardening and vulnerability assessment; contamination, thermal and structural control; lubrication and surface phenomena. Microelectromechanical systems (MEMS) for space applications; laser micromachining; laser-surface physical and chemical interactions; micropropulsion; micro- and nanosatellite mission analysis; intelligent microinstruments for monitoring space and launch system environments.

Space Science Applications Laboratory: Magnetospheric, auroral and cosmic-ray physics, wave-particle interactions, magnetospheric plasma waves; atmospheric and ionospheric physics, density and composition of the upper atmosphere, remote sensing using atmospheric radiation; solar physics, infrared astronomy, infrared signature analysis; infrared surveillance, imaging and remote sensing; multispectral and hyperspectral sensor development; data analysis and algorithm development; applications of multispectral and hyperspectral imagery to defense, civil space, commercial, and environmental missions; effects of solar activity, magnetic storms and nuclear explosions on the Earth's atmosphere, ionosphere and magnetosphere; effects of electromagnetic and particulate radiations on space systems; space instrumentation, design, fabrication and test; environmental chemistry, trace detection; atmospheric chemical reactions, atmospheric optics, light scattering, state-specific chemical reactions, and radiative signatures of missile plumes.



The Aerospace Corporation
2310 E. El Segundo Boulevard
El Segundo, California 90245-4609
U.S.A.